AD-A127 116 ELECTROPLATING OF REFRACTORY METALS AND ALLOYS FROM FLUORIDE MELT(U) RENSSELAER POLYTECHNIC INST TROY N Y DEPT OF CHEMISTRY R A BAILEY 22 MAR 83 ARO-15916.2-MS 1/

UNCLASSIFIED DAAG29-79-C-0035 F/G 13/8 NL

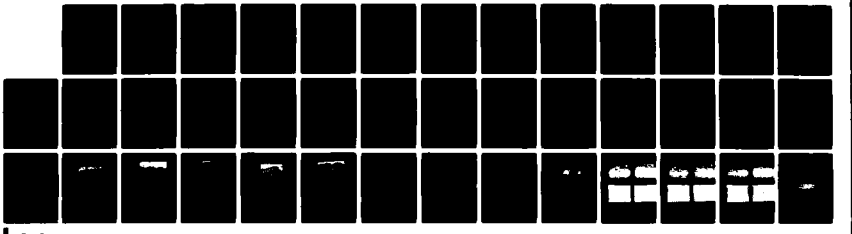

END
DATE FILMED
5 83
DTIC

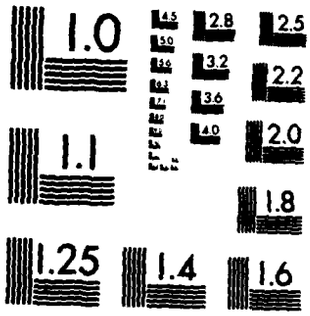

Unclassified

SECURITY CLASSIFICATION OF THIS PAGE (When Data Entered)

ARO 15916.2-MS

AD A127116

DTIC FILE COPY

REPORT DOCUMENTATION PAGE

READ INSTRUCTIONS BEFORE COMPLETING FORM

1. REPORT NUMBER: Final Report #1	2. GOVT ACCESSION NO.: AD-A127116
3. RECIPIENT'S CATALOG NUMBER:	
4. TITLE (and Subtitle): Electroplating of Refractory Metals and Alloys From Fluoride Melt	5. TYPE OF REPORT & PERIOD COVERED: Final Report - Jan 80-Dec 83
	6. PERFORMING ORG. REPORT NUMBER:
7. AUTHOR(s): R. A. Bailey	8. CONTRACT OR GRANT NUMBER(s): DAAG29-79-C-0035
9. PERFORMING ORGANIZATION NAME AND ADDRESS: Rensselaer Polytechnic Institue, Chemistry Department, Troy, New York 12181	10. PROGRAM ELEMENT, PROJECT, TASK AREA & WORK UNIT NUMBERS:
11. CONTROLLING OFFICE NAME AND ADDRESS: U. S. Army Research Office, Post Office Box 12211, Research Triangle Park, NC 27709	12. REPORT DATE: March 22, 1983
	13. NUMBER OF PAGES:
14. MONITORING AGENCY NAME & ADDRESS (if different from Controlling Office)	15. SECURITY CLASS. (of this report): Unclassified
	15a. DECLASSIFICATION/DOWNGRADING SCHEDULE:

16. DISTRIBUTION STATEMENT (of this Report)

Approved for public release; distribution unlimited.

17. DISTRIBUTION STATEMENT (of the abstract entered in Block 20, if different from Report)

A

18. SUPPLEMENTARY NOTES

The view, opinions, and/or findings contained in this report are those of the author(s) and should not be construed as an official Department of the Army position, policy, or decision, unless so designated by other documentation

19. KEY WORDS (Continue on reverse side if necessary and identify by block number)

20. ABSTRACT (Continue on reverse side if necessary and identify by block number)

Reduction of Cr(III) in molten LiF-NaF-KF proceeds by the process

$$Cr(III) \underset{\text{slow}}{\overset{\text{quasi-reversible}}{\rightleftharpoons}} Cr(II) \underset{\text{slow}}{\overset{\text{quasi-reversible}}{\rightleftharpoons}} Cr(0)$$

Cr(II): insoluble below 900°C

Best conditions for metal electroplating is between 900 and 1000°C, when dendrite

DD FORM 1 JAN 73 1473 EDITION OF 1 NOV 65 IS OBSOLETE

UNCLASSIFIED

SECURITY CLASSIFICATION OF THIS PAGE (When Data Entered)

20. formation is eliminated in pure melts. Grain size remains large, however. A variety of other metal fluoride additives increased dendrite formation or, in the case of NiF_2, increased the void content of the plate. Use of $NaSiF_7^{-2}$ produced very smooth but very brittle alloy deposits. NbF_7^{-2} and TaF_7^{-2} showed 3-step, irreversible reductions that also changed in details with temperature.

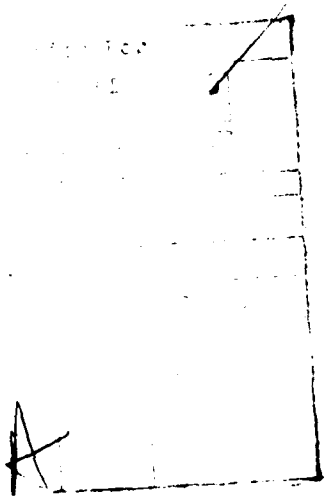

This project involved an investigation of electroplating of refractory metals, chiefly chromium, from the molten LiF-NaF-KF ternary eutectic. Initial objectives were to establish the mechanisms of the electro-reduction processes, especially for chromium, to explore the conditions that might lead to thick, coherent, electrodeposited coatings of chromium, and to examine the effects of co-deposits of other elements on the properties of the deposits. The electrochemical behavior of other refractory metals, tantalum and niobium, was also examined.

Apparatus and Techniques

Electroplating and electrochemistry were carried out in an apparatus shown in Fig. 1. This was built first of stainless steel, later replaced by Hasteloy-X. A 3-inch gate-valve permitted electrodes to be inserted and removed without opening the system to the atmosphere; a purified argon blanket was maintained at all times. The melt was contained in a nickel crucible.

Electrodes for electroplating experiments consisted of a refractory metal anode and a steel or copper cathode. The cathodes were polished and cleaned by brief etching in acid. Normally, the cathode was welded to a stainless steel support attached to a stainless steel tube that was inserted through an O-ring gland. The other electrode was suspended from a steel wire concentric with the steel tube and insulated from it by alumina insulators which did not, however, extend below the bottom of the tube, which was well above the melt surface. Normally, a nickel extension wire was welded to the steel wire to ensure that no other metal would be anodized in the event that the suspension contacted the melt (Nickel is noble with respect to chromium here). Various sources of chromium metal were used, ranging from 99.9% to 99.95% purity. No obvious relation of plating characteristics to anode purity could be discerned, but the more highly pure metal was used for most critical experiments.

The alkali fluoride salts were reagent grade, stored separately under vacuum at 150°C for at least a week before use. The eutectic composition was then made up, pre-melted under argon in a separate apparatus, and filtered through multiple layers of platinum gauze welded over a hole in a nickel crucible to remove black particulate material that was usually present. In most cases, each batch of melt was pre-electrolyzed using a steel cathode and vitreous carbon anode at about 1.5 V before being cooled and trasnferred to the electrochemical cell.

Electrochemical electrodes consisted of a platinum foil quasi-reference electrode, a vitreous carbon auxillary electrode, and a platinum disc or needle working electrode for chronopotentiometry and cyclic voltammetry, respectively.

Electroplating was carried out at constant current, either continuously, or with current reversal. Plate quality was evaluated by Prof. I. Ahmad, Benet Weapons Laboratory, Watervliet Arsenal, who provided microhardness measurements, and microphotographs of polished cross sections.

The controlled potential cyclic voltammeter used was designed and built in this laboratory. With this instrument, scan rates from 0.01 to 80V/sec are available and cell currents up to 500 mA can be measured. A constant current power supply (HP model 6212A) was used for chronopotentiometry. Waves were recorded by means of either a Tektronix type 564 stroage oscilloscope or an Omnigraphic series 2000 X-Y recorder.

As the soluble chromium compound, either CrF_3 or K_3CrF_6 (made by a modification of the procedure of Christensen (1)) was used. K_2TaF_7 and K_2NbF_7 were sources of tantalum and niobium for measurements of these elements.

Chromium Electrochemistry

Cyclic voltammograms and chronopotentiograms for reduction of Cr(III) in the fluoride eutectic are shown in Fig. 2 at different temperatures. Both cyclic voltammograms and chronopotentiograms were run over a temperature

range of about 600 to 1000°C and a Cr(III) concentration of 0.07 to 0.13 mol/l. Two reduction and two oxidation steps are evident. The first reduction step and the second oxidation step became indistinct at lower temperatures and lower scan rates, eventually almost merging with the others. This is mainly due to the tendency of the second reduction and first oxidation peaks to shift anodic with decreasing scan rates, decreasing temperature and increasing concentration of Cr(III). The shape of the first reduction wave in cyclic voltammetry is not in the form of a peak, but is sigmoidal at lower scan rates. However, at high scan rates it develops into a peak. Therefor, it is qualitatively apparent that the first recution step is not a simple reversible, diffusion controlled reduction process.

The data that can be extracted from these results are shown in Figs. 3-6 and Tables 1-5. When these results are compared to the standard criteria for reaction mechanisms (2-6), as in Table 6, both reactions are found to be quasi-reversible. The first reduction is a one-electron step, producing an insoluble product below about 900°C, but fitting the criteria for a soluble product above this temperature (3). The second step is a 2-electron reduction to chromium metal.

However, an additional complication is the disproportionation of the chromium according to the following reaction,

$$3Cr(II) \rightarrow 2Cr(III) + Cr(metal)$$

as pointed out by Mellors and Senderoff (7) and Redman (8). We also found that 8 wt % of CrF_2 added to molten FLINAK for electrolysis did disproportionate and small amounts of Cr metal deposited on the surface of the Ni container after a week's experiment. The elctrochemical results for a solution made from CrF_2 were qualitatively the same as when Cr(III) was used. However, it is believed that this disproportionation reaction is so slow that it cannot be detected within the range of the scan rates used in our experiment. Since our experiment has been carried out at a relatively high

temperature (600-1000°C) and the effects of convection in the melt become significant, reproducible measurements cannot be obtained at lower scan rates (≤ 1.0V/sec) and lower current density where the detection of a catalytic reaction might be feasible.

Ratios of the transition times of the second reduction to the first exidation step, τ_{2f}/τ_{1r}, obtained at different temperatures are listed in Table 7. At lower temperatures this ratio is very close to unity, but decreases with increasing temperature. Since the second reduction step has been found to be a quasi-reversible reduction of Cr(III) to Cr metal, this value should be unity. Possibly, an alloy formation of deposited Cr metal with the Pt electrode might be responsible for the reduction of the ratio at higher temperatures.

Our results are in reasonable agreement with voltammetric measurements in CrF_2 in $LiF-BeF_2--ZrF_4$ at 500°C by Manning and Dale (9) who found that the reduction of Cr(II) to Cr metal is a quasi-reversible process.

The diffusion coefficient of the electroactive species, D, can be estimated from the Sand equation:

$$i_o \tau^{\frac{1}{2}} = \frac{nFC(\pi D)^{\frac{1}{2}}}{2} \qquad (2)$$

where i_o is the current density, i_p the peak current, τ the transition time, c the concentration of electroactive species and the remaining terms have their usual significance. The result is shown plotted as the logarithm against the reciprocal of absolute temperature in Figure 8; the result is a straight line. The diffusion coefficients of Cr(III) obtained in molten FLINAK seem to be low (983°C: 1.84×10^{-6}, 893°C: 1.19×10^{-6}, 804°C: 0.95×10^{-6}, 716°C: 0.59×10^{-6}, 612°C: 1.84×10^{-6} cm^2/sec), despite some uncertainty (± 20%) mainly in the surface area of the working electrode and the concentration of Cr(III). The activation energy for the diffusion of Cr(III) calculated from the slope in Figure 7 is 9.5 kcal/mol. Similar small diffusion coefficients

and large activation energies have been found for some refractory and transition metals in molten FLINAK (10,11,12,13) (exceptions are Nb and Ta (14,15)). This is probably due to higher viscosity of FLINAK (at 454°C, > 10 m Pa.S) (16) and to the existence of a large and stable complex anion like CrF_6^{3-} in the melt.

Analysis of melt samples taken during and after electroplating runs gave an average oxidation state for the chromium in the melt of 2.6. That is, nearly half of the chromium is present in the +2 state during plating conditions. Coulombic measurements of the anodic dissolution of chromium metal, in which weight loss measurements were compared to amount of current passed, showed that the average oxidation state of chromium produced in the melt was about 2.7, although probably varying with temperature and perhaps current density.

The quasi-reversible electrochemistry suggests that the reduction processes involve metal ions that are not freely accessible, and that might be involved in the formation of stable complexes and/or cluster compounds (17). Certainly Cr(III) is a very strong complex forming ion, especially with hard ligands such as F^-, while Cr(II) is known to form metal-metal bonds in other media.

Chromium Electroplating

An extensive study of the variation of plating conditions on the nature of the plate was carried out, with results that can be summarized as follows:

1. Temperature: smoothest deposits were obtained between 900°C and 1000°C. At lower temperatures, extensive dendrite formation occurred. Higher temperature deposits also exhibited increased dendrite formation, although of a somewhat different physical form (needles, as opposed to flat, leaf-like forms). The change in nature of the deposit near 900°C is correlated with changes in the electrochemical mechanism; specifically, the change from an intermediate consistent with an insoluble product to a soluble one.

2. Melt Compositions: little effect of chromium content of the melt on plate characteristics could be noted above about 6 wt % CrF_3. Initial deposition was dependent on time of electrolysis; however, no deposit could be obtained until after about 5 hrs at 30 ma cm^{-2}. This was caused by the fact that during this initial time most of the current was used to reduce Cr^{+3} to Cr^{+2}; only after the latter reached a sufficient concentration was metal produced. If Cr^{+2} were added to the melt as CrF_2 initially, plating began at once. Plating was also attempted in NaF-KF melts, to see if the absence of Li^+, which would tend to be destabilizing to complexes or cluster compounds, would improve plating properties. Qualitatively there seemed to be a reduction of dendrite formation in Li^+-free melts, but this was a slight effect. The greater volatility of the NaF-KF eutectic limited work in this medium.

3. Current Variables: below about 40 ma cm^{-2}, little change could be noted from changing current density unless very low values (< 5 ma cm^{-2}) were used. Even this had little effect on dendrite formation below 900°C; but very small currents seemed to lead to somewhat smaller crystallities in the deposit. Various experiments employing current interruption, current reversal, solution stirring (through argon bubbling) and vibration of the cathode lead to some reduction of dendrite formation, but had little effect on the plate above 900°C.

4. Substrates: most specimens were plated on type 304 stainless steel. Some plating was done on copper, but with much poorer results. The tendency on copper was for the nucleation of smaller numbers of larger crystals. Other experiments were carried out on nickel, nickel plated steel, or nickel plated copper. In all cases, smooth, apparently fine grained deposits formed initially, but in thicker layers there was no obvious difference from the steel samples. Microphotographs of cross-sections were not different from those on steel- e.g., Figs. 8 and 9.

5. Characterization of deposits: hardness tests were done on cross-sections of deposits. Values as shown on Figs. 10, 11, 12 show that the deposits are relatively soft, as would be expected for reasonably pure metal. Etched cross-sections are shown in Figs. 8, 9, 13. As can be sceen, crystal size is relatively large, and voids tend to occur between some of the large crystals, especially for deposits obtained near 900°C. Consequently, deposits are mechanically unsatisfactory. Although the coating is complete and individual grains apparently of good characteristics, coatings with substrate dissolved away easily fracture.

6. Effects of other metal ions in the bath: Small amounts (< 1 wt % to 3 wt %) of other metal fluorides were added to the fluoride bath in an effort to modify the crystal growth characteristics of the plate. Because the second chromium reduction step occurs at a relatively negative potential, many possible additives are preferrentially deposited, but at low concentrations could be expected to co-deposit with the chromium metal. Some effects were noted, most unfortunately deleterious.

Nickel, although deposited much more easily than chromium, caused a market change in the appearance of the chromium deposit until the nickel content was exhausted. (Values less than 0.1 wt % NiF_2). At 1 wt % NiF_2, the granular appearance of the plate was changed to a smoother consistency, with crystals appearing to be flat rather than columnar. The deposit itself, however, showed excessive voids and irregularities (Fig. 14). As the Ni, content decreased, successive plates exhibited very large flat dendrites (Fig. 15).

Other metal ions when present at 1 wt % concnetrations either result in poorly adherent coatings (e.g., FeF_2) or enhance dendrite formation, sometimes spectacularly. Dendrites can range from large thin plates to very long needles (MnF_2), Fig. 16.

Addition of 10% Na_2SiF_6 to the melt permits deposition of very smooth deposits of a chromium-silicon alloy. As silicon deposits preferrentially, the Si content does not remain constant, and as Si is depleted in the melt, excellent octehedral crystals of chromium are formed. This alloy is extremely hard and brittle, frequently showing macroscopic stress cracks that develop as the steel substrate cools from the 900°C plating temperature. A summary of these additive effects is given in Table 8.

Other Metals: Electrochemistry

Representative electrochemical data for tantalum and niobium in the ternary fluoride melt are shown in Fig. 17 and 18. These systems were investigated earlier by Senderoff and Mellors, (14,15); we have repeated this work primarily to examine temperature effects, as the earlier electrochemical studies were not made at the temperatures providing optimum plating conditions. In both cases, we agree generally with the previous conclusions, i.e., the reductionsare multi-step processes, and not over-all reversible. However, voltammogams for the reduction of NbF_7^{2-} indicate that none of the three steps, assigned by Senderoff and Mellors to the reactions

$$[NbF_7]^{2-} + e^- \rightarrow [NbF_{(7-x)}]^{(3-x)-} + XF^-$$

$$[NbF_{(7-x)}]^{(3-x)-} + 3e^- \rightarrow NbF + (6-x)F^-$$

$$NbF + e^- \rightarrow Nb^\circ$$

are reversible; neither can we confirm that NbF (i.e., Nb^{+1}) is the correct oxidation state for the second intermediate. Further, there is an indication of a third reduction step in addition to the two previously suggested.

$$([TaF_7]^{-2} + 3e^- \rightarrow TaF_2$$

$$TaF_2 + 2e^- \rightarrow Ta^\circ)$$

in the r[illegible]ion $[TaF_7]^{-2}$. Both elements show changes in the details of the electrochemistry with temperatures.

Publications Resulting from this project

1. The Electrochemistry of Chromium in Molten LiF-NaF-KF Eutectic; T. Yoko and R. A. Bailey, J. Electrochem. Soc., submitted for publication.

2. Electrochemical Studies of Chromium in Molten LiF-NaF-KF, paper presented at the 159th Meeting of the Electrochemical Society, Minneapolis, Minnesota, May, 1981, by T. Yoko and R. A. Bailey.

3. Electrochemical Studies of Chromium in Molten LiF-NaF-KF, paper presented to the Tri-Service Gun Tube Wear and Erosion Symposium, Dover, N.J., Oct. 1982, by T. Yoko and R. A. Bailey.

4. Electrochemistry of Nibioum in Molten FLINAK, paper to be presented at the First International Symposium on Molten Salt Chemistry and Technology, Kyoto, Japan, April, 1983, by T. Yoko and R. A. Bailey.

5. Electroplating of Chromium in Molten FLINAK, paper to be presented at the First International Symposium on Molten Salt Chemistry and Technology, Kyoto, Japan, April, 1983, by. T. Yoko and R. A. Bailey.

Participating Scientific Personnel

R. A. Bailey - Principal Investigator

A. A. Nobile - Postdoctoral Research Associate

T. Yoko - Postdoctoral Research Associate

Sen Lin Du - Research Associate

Laura Babcock - Undergraduate assistant (work performed on this project will be presented as a senior thesis toward the B.Sc. degree, May, 1983)

Several undergraduate students participated as technical help.

References

1. O. T. Christensen, J. Pract. Chem., 35, 161 (1887).

2. I. J. Bard and L. R. Faulkner, Electrochemical Methods - Fundamentals and Applications, John Wiley and Sons, New York, 1980, Ch. 7 and 11.

3. D. D. MacDonald, Transient Techniques in Electrochemistry, Plenum Press, New York, 1977, Ch. 5.

4. A. A. Bond, Modern Polarographic Methods in Analytical Chemistry, Marcell Dekker Inc., New York, 1980, Ch. 3 and 5.

5. T. Berzins and P. Dalahay, J. Amer. Chem. Soc., 75, 4205 (1953).

6. R. S. Nicholson, Anal. Chem., 37, 1406 (1965).

7. G. W. Mellors and S. Senderoff, Applications of Fundamental Thermodynamics to Metallurgical Processes, G. R. Fitterer, ed., Gordon and Breach, New York, 1967, p. 81.

8. J. O. Redman, O. R. N. L. 2626 M.S.R.P., Q.P.R. 94 (1958).

9. D. L. Manning and J. M. Dale, Molten Salts, G. Mamantov, ed., Marcell Dekker Inc., New York, 1967, p. 563.

10. D. L. Manning, J. Electroanal. Chem., 6, 227 (1963).

11. D. L. Manning, J. Electroanal. Chem., 7, 302 (1964).

12. F. R. Clayton, G. Mamantov and D. L. Manning, J. Electrochem. Soc., 120, 1193 (1973).

13. F. R. Clayton, G. Mamantov and D. L. Manning, J. Electrochem. Soc., 121, 86 (1974).

14. S. Senderoff, G. W. Mellors, and W. J. Reinhart, J. Electrochem. Soc., 112, 840 (1965).

15. S. Senderoff, and G. W. Mellors, J. Electrochem. Soc., 113, 66 (1966).

16. K. Tørklep, and H. A. Øye, J. Chem. Eng. Data, 25, 16 (1980).

17. D. Inman and S. H. White, J. Appl. Electrochem., 8, 375 (1978).

Table 1

Concentration Dependence of Peak Potentials and Quarter-Wave Potentials. Scan Rate (voltammetry) 2.0V sec^{-1}; Current Density (chronopotentiometry) 45.9 x 10^2 mAm^{-2}; Temperature 983°C

Concentration of Cr (III), mole l^{-1}	Ep/V		$E_{\tau/4}$/V	
	1st wave	2nd wave	1st wave	2nd wave
0.07	-0.86	-0.774	-	-
0.08	-0.164	-0.762	-0.32	-0.782
0.10	-0.156	-0.746	-0.259	-0.792
0.11	-0.192	-0.734	-0.202	-0.764
0.12	-	-	-0.206	-0.752

Table 2

Scan Rate Dependence of Peak Potentials (voltammetry) and Current Density Dependence of Quarter-Wave Potential (chronopotentiometry). Concentration of Cr (III); 0.11 mole l^{-1}, 983°C

Scan Rate, V sec^{-1}	Ep/V		Current Density mAm m^{-2}	$E_{\tau/4}/4$	
	1st wave	2nd wave		1st wave	2nd wave
1.0	-0.126	-0.738	33.2	-0.135	-0.610
2.0	-0.152	-0.749	35.8	-0.145	-0.616
5.0	-0.162	-0.786	38.4	-0.156	-0.628
8.0	-0.173	-0.796	40.9	-0.178	-0.637
10.0	-0.186	-0.815	43.5	-0.194	-0.646
20.0	-0.234	-0.857	46.0	-0.244	-0.656

Table 3 Temperature dependence of the ratio of the transition time of the first to the second reduction step, τ_{2r}/τ_{1r} (concentration of Cr(III) = 0.09 mol.l^{-1}).

Temp (°C)	983	893	804	716	612
τ_{2r}/τ_{1r}	8.0	8.6	9.3	11.3	13.4

Table 4 Ratio of the forward to the reverse transition time for the first wave at different temperatures (Concentration of Cr(III) = 0.13 mol. ℓ^{-1}).

Temp. (°C)	Current Density (10^2.mA.m^{-2})	Transition time Forward τ_f (sec)	Reverse τ_r (sec)	τ_f/τ_r
983	51.0	0.102	0.039	2.6
	40.8	0.156	0.047	3.3
893	46.0	0.067	0.071	0.93
	35.8	0.110	0.098	1.1
804	30.7	0.157	0.126	1.2
	25.6	0.201	0.193	1.0
716	25.6	0.114	0.112	1.0
	20.5	0.186	0.169	1.1
612	20.6	0.119	0.123	0.97
	18.0	0.158	0.150	1.1

Table 5 Ratios of the anodic to the cathodic peak current i_{ap}/i_{cp}, peak potentials and their peak separation at different scan rates (concentration of Cr(III) = 0.11 $mol.l^{-1}$).

Temp (°C)	Scan rate ($V.sec^{-1}$)	i_{ap}/i_{cp}	E_{cp} (V)	E_{ap} (V)	$E_{cp}-E_{ap}$ (V)
983	20	1.27	-0.286	-0.091	-0.377
	10	1.18	-0.236	-0.085	-0.321
	8	1.12	-0.226	-0.075	-0.301
	5	1.02	-0.213	-0.070	-0.283
	2	0.95	-0.186	-0.051	-0.237
	1	0.92	-0.157	-0.049	-0.201
					-0.253*
893	50	1.34	-0.339	-0.206	-0.545
	20	1.22	-0.226	-0.135	-0.351
	10	1.17	-0.199	-0.109	-0.308
	5	1.22	-0.173	-0.091	-0.264
	1	1.02	-0.152	-0.073	-0.225
					-0.234*

*: Theoretical values calculated based on the reversible process (as n = 1).

E_{ap}, E_{cp} : Anodic and cathodic peak potential, respectively.

Table 6 Comparison of the results obtained for the first reduction step with the diagnostic criteria for typical electrode processes.

Electrode process	$i_p/V^{1/2}$ vs. V	$i.\tau^{1/2}$ vs. i	ipa/ipc vs. V	Ep vs. V	$E_{\tau/4}$ vs. i	$E_{\tau/4}$ vs. C	τ_f/τ_r vs. i
Observed	const.	const.	incr.	cathodic	cathodic	anodic	1 a) 3 b)
Reversible	const.	const.	1 c) > 1 d)	const.	const.	const.	1 c) 3 d)
Quasi-rev.	const.	const.	———	cathodic	cathodic	anodic	1 c) 3 d)
Irrev.	const.	const.	0	cathodic	cathodic	anodic	0 or 1 c) 0 or 3 d)
Cr.Er	decr.	decr.	incr. from 1 at low V	anodic	———	———	3
Er.Cr	const.	const.	decr. from 1 at low V	cathodic	cathodic	anodic	incr.
Catalytic	*	incr. from 1	*	anodic or const.	anodic	———	———

Cr.Er : Reversible chemical reaction preceding a reversible charge transfer.

Er.Cr : Reversible charge transfer followed by a reversible chemical reaction.

* : Decreasing at low V and constant at high V.

a) : At 983 °C ; b) : Below 893 °C.

c) : Insoluble product ; d) : Soluble product.

Table 7 Temperature dependence of the ratio of the transition time of the second reduction to the first oxidation step, τ_{2f}/τ_{1r} (concentration of Cr(III) = 0.09 mol.l^{-1}).

Temp(°C)	983	893	804	716	612
τ_{2f}/τ_{1r}	0.58	0.66	0.86	0.98	1.1

Table 8

Effect of Metallic Additives of Chromium Plating

Additive	Nature of Deposit
NiF_2, 1%	smooth, small crystals, voids (Fig. 15)
NiF_2, < 0.5%	flat dendrites (Fig. 16)
FeF_2, 1%	no adherent deposit
MnF_2, 1%	large needle-like dendrites (Fig. 17)
Na_2SiF_6, 5-10%	smooth, hard chromium silicide deposit; at low SiF_6^{-2} content, Cr crystals begin to form
$NaBF_4$, 5 wt%	no coherent deposit; separate metal crystals form in substrate
K_2TaF_7 1-3%	no obvious effect
$NaBF_4$, 1 wt%	dendritic coating only on side of cathode facing anode
AlF_3, 10%	increased dendrite formation

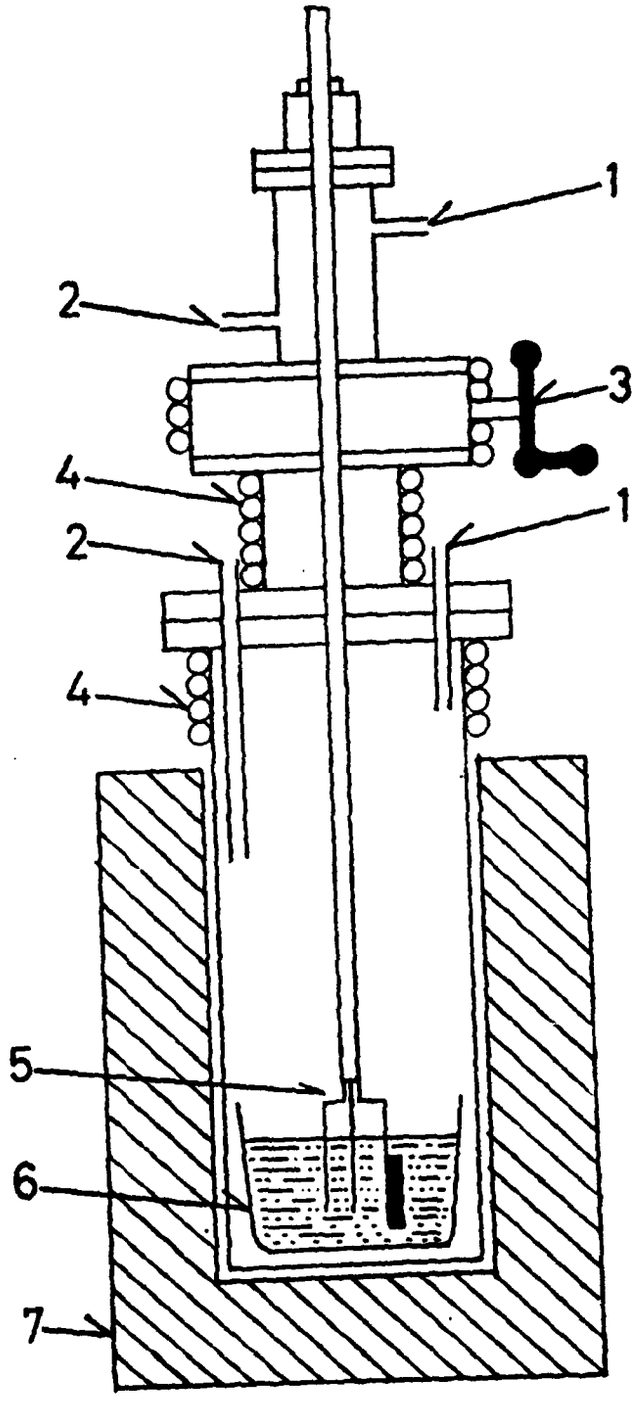

Figure 1 Schematic diagram of the electrochemical cell; 1: gas outlet; 2: gas inlet; 3: gate valve; 4: water cooling coil; 5: electrodes; 6: Ni crucible and molten salt; 7: furnace.

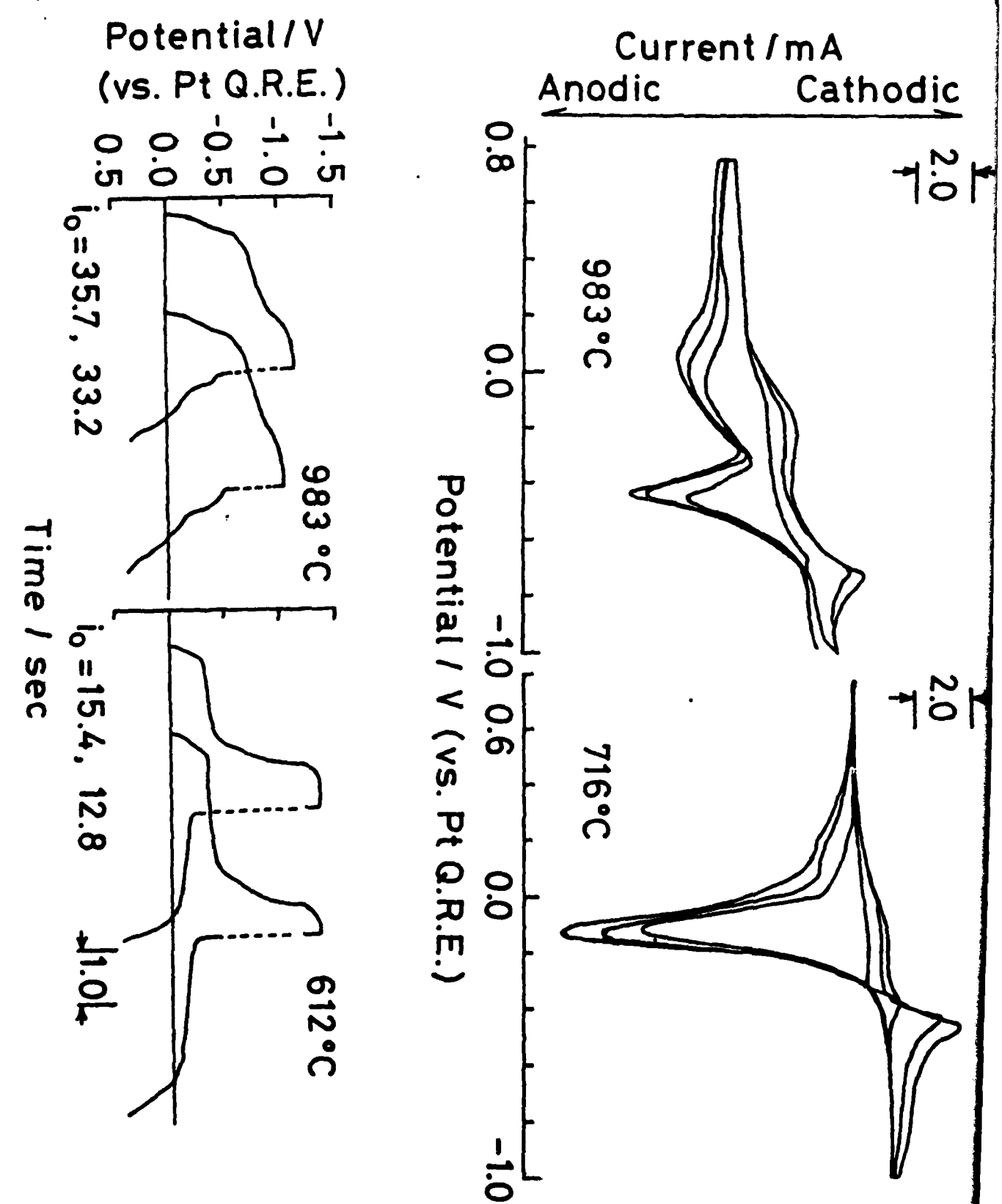

Figure 2 Cyclic voltammograms for the reduction of Cr(III) in molten FLINAK (scan rate: 8.0, 5.0 and 1.0V sec^{-1}; concentration of Cr(III) = 0.10 $mol.l^{-1}$)

Upper:

Lower: Chronopotentiograms for the reduction of Cr(III) in molten FLINAK (concentration of Cr(III) = 0.10 $mol.l^{-1}$; i_o = current density/10^{-2} $mA.m^{-2}$).

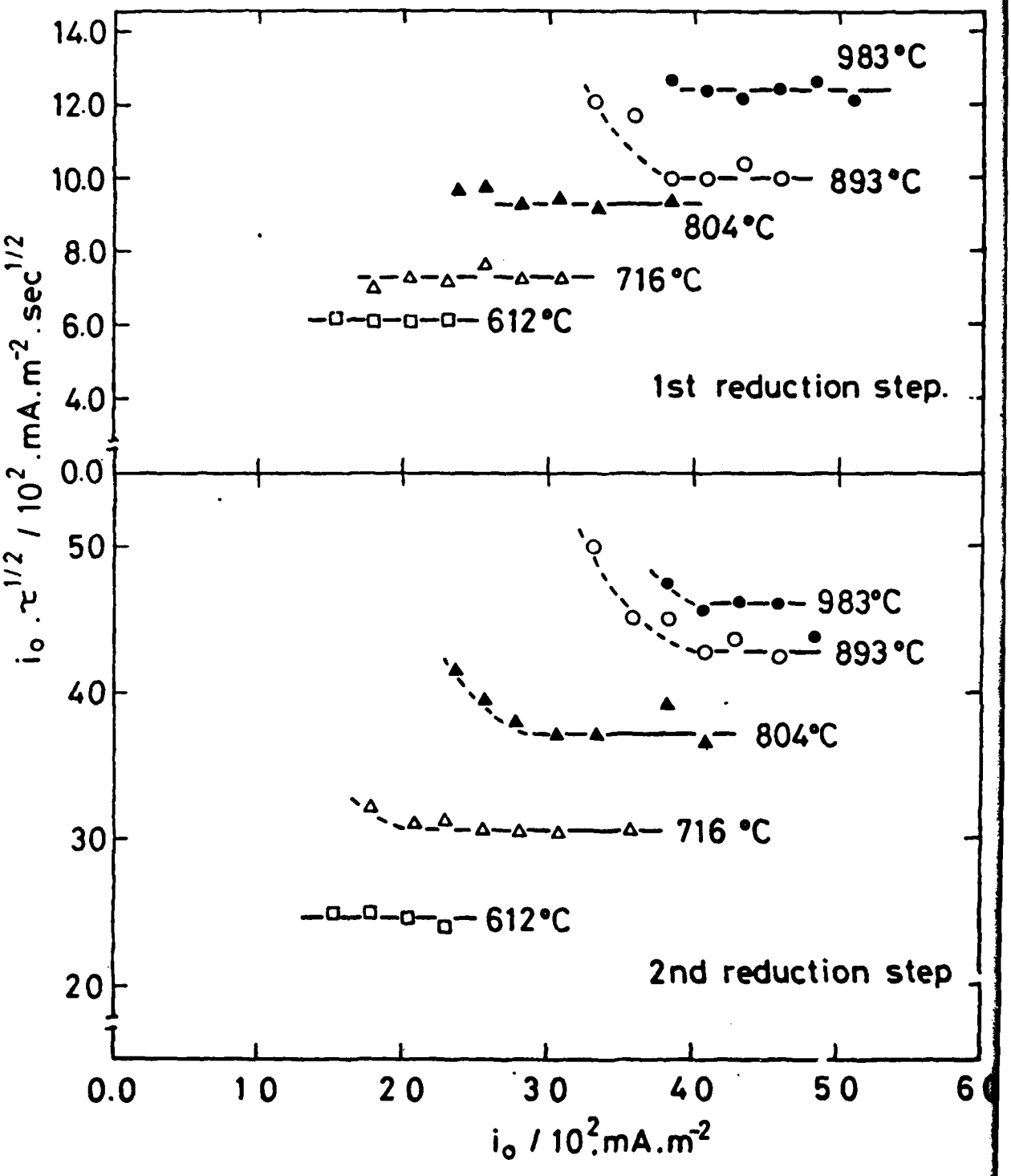

Figure 3 Plots of $i_o \tau^{\frac{1}{2}}$ vs. i_o for the first and second reduction steps of Cr(III) in molten FLINAK (concentration of Cr(III) = 0.11 mol l^{-1}; Pt working electrode area = 0.98 x $10^{-4} m^2$).

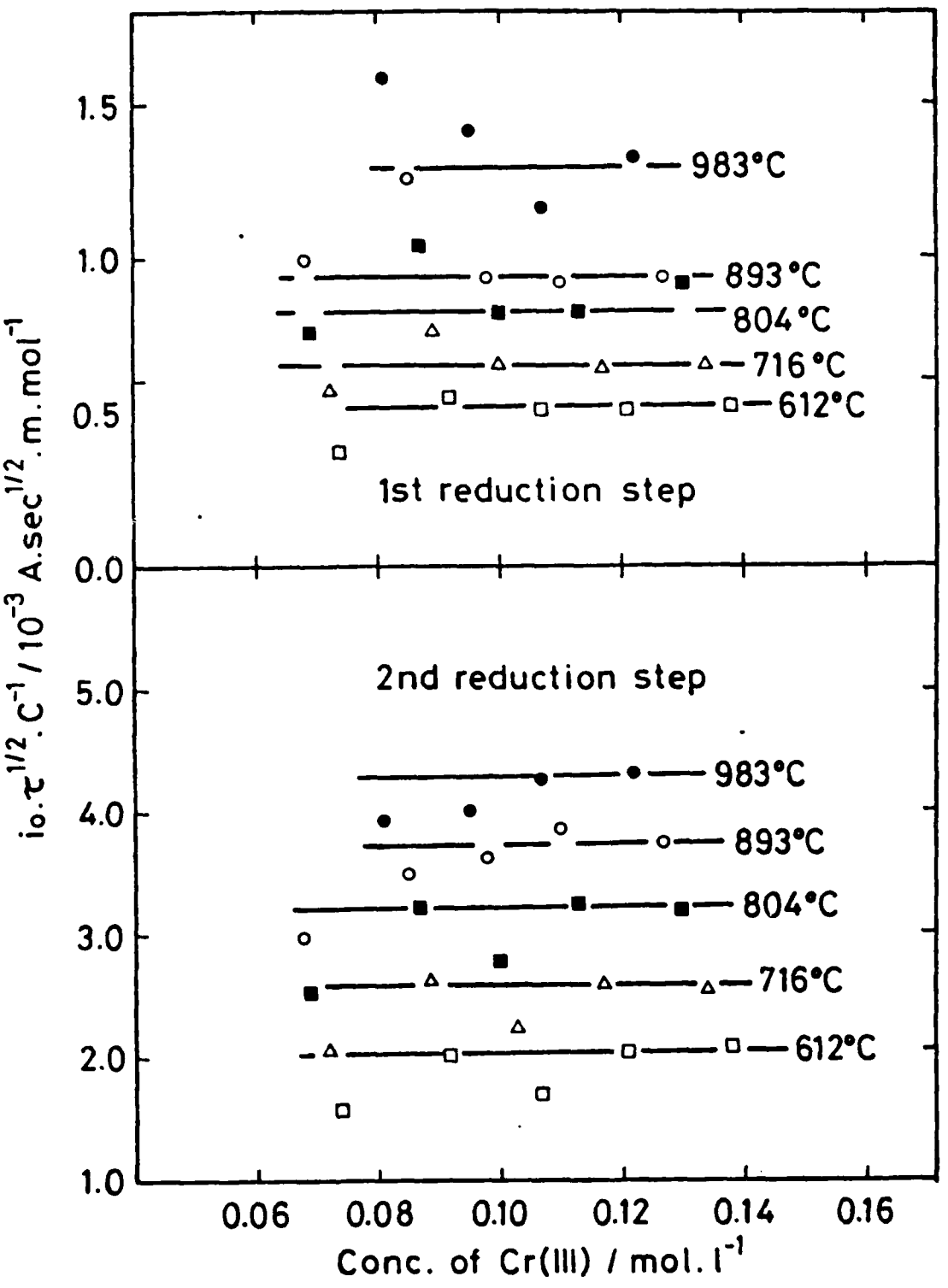

Figure 4 Plots of $i_o \tau^{\frac{1}{2}}/C$ vs. C (concentration of Cr(III), for the first and second reduction steps.

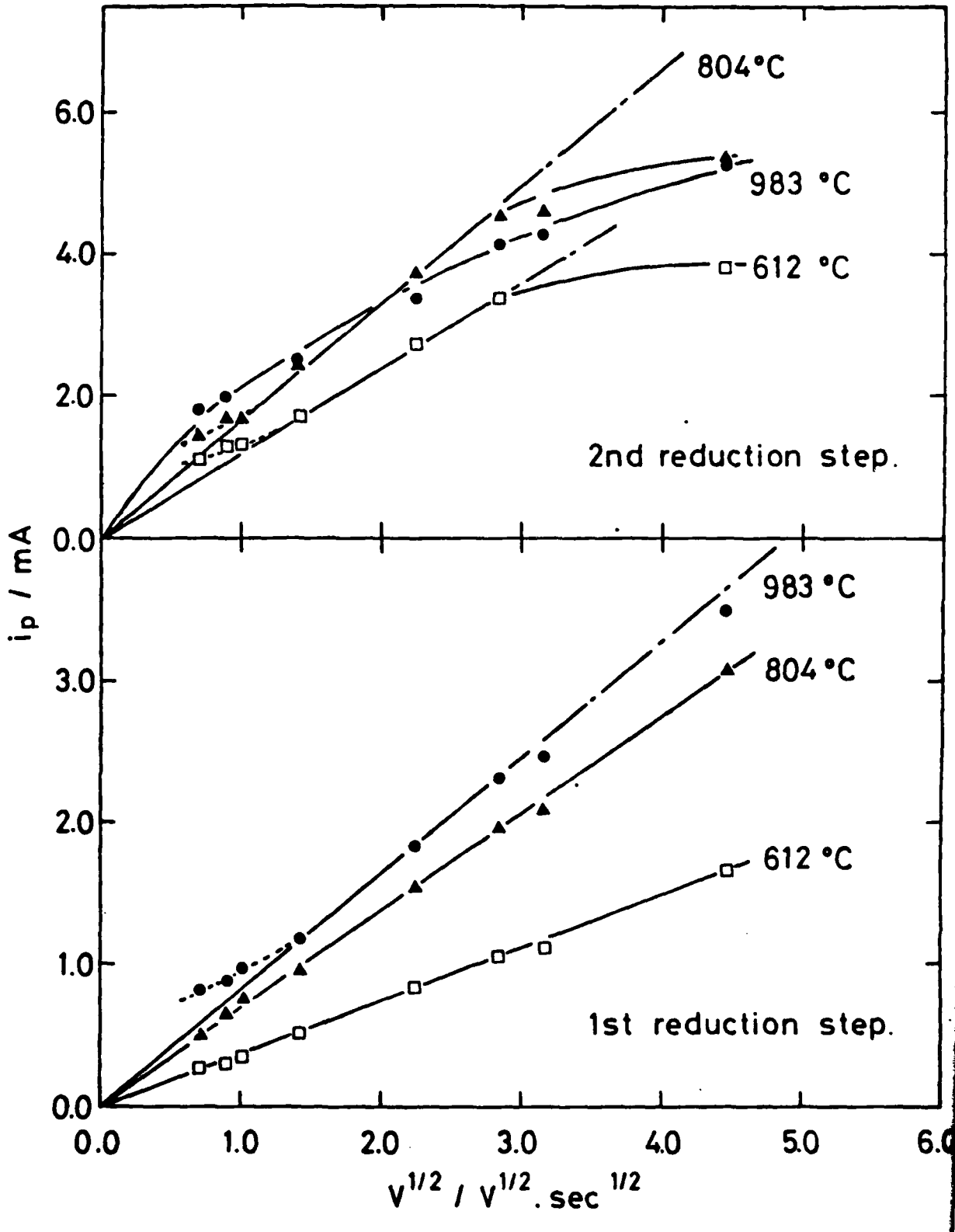

Figure 5 Plots of i_p vs. V for the first and second reduction steps of Cr(III) in molten FLINAK (concentration of Cr(III) = 0.11 mol.l^{-1}; Pt micro-electrode area = 2.02 x $10^{-6}m^2$).

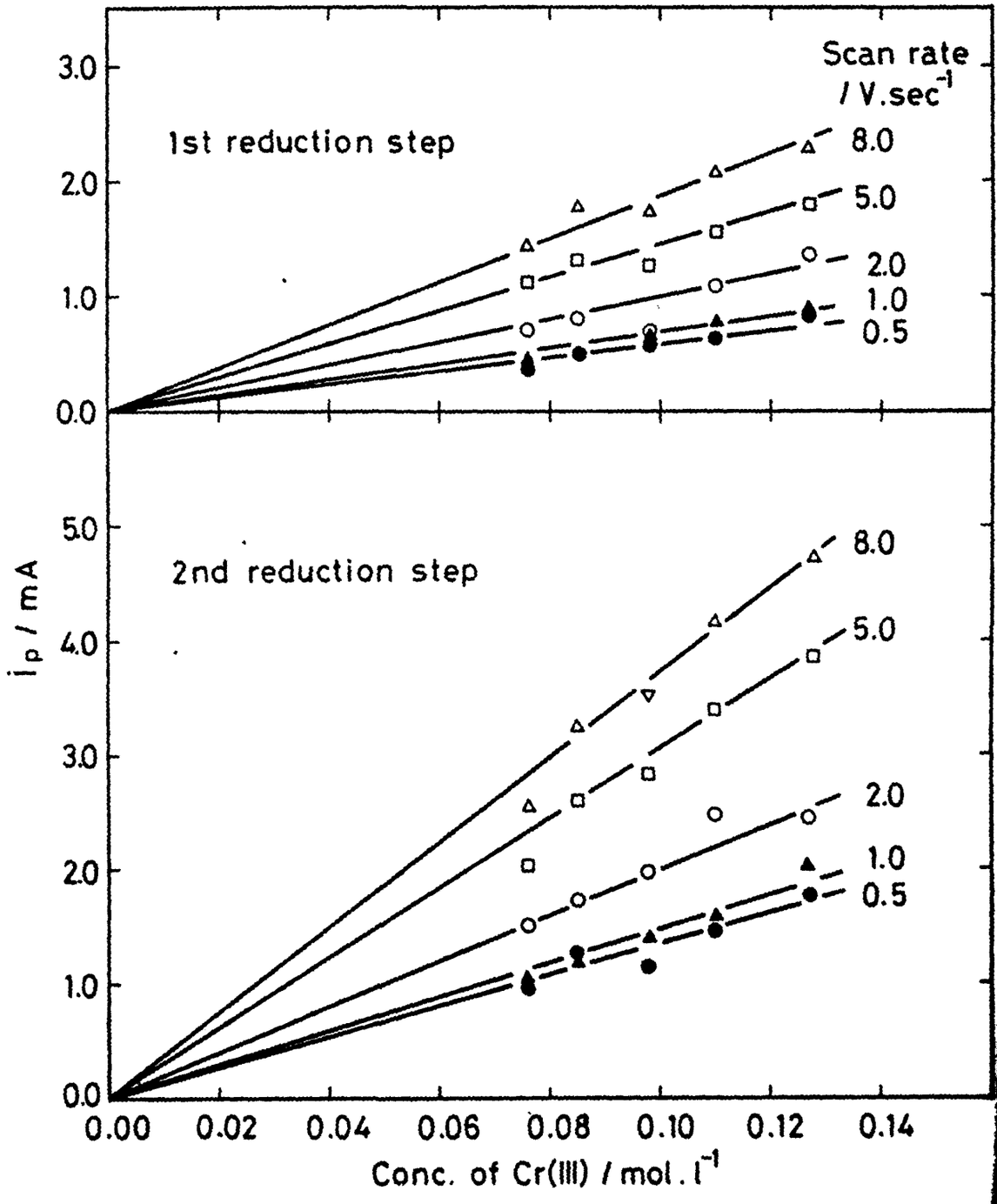

Figure 6 Plots of peak current i_p vs. concentration of Cr(III) for the first and second reduction steps at 893°C.

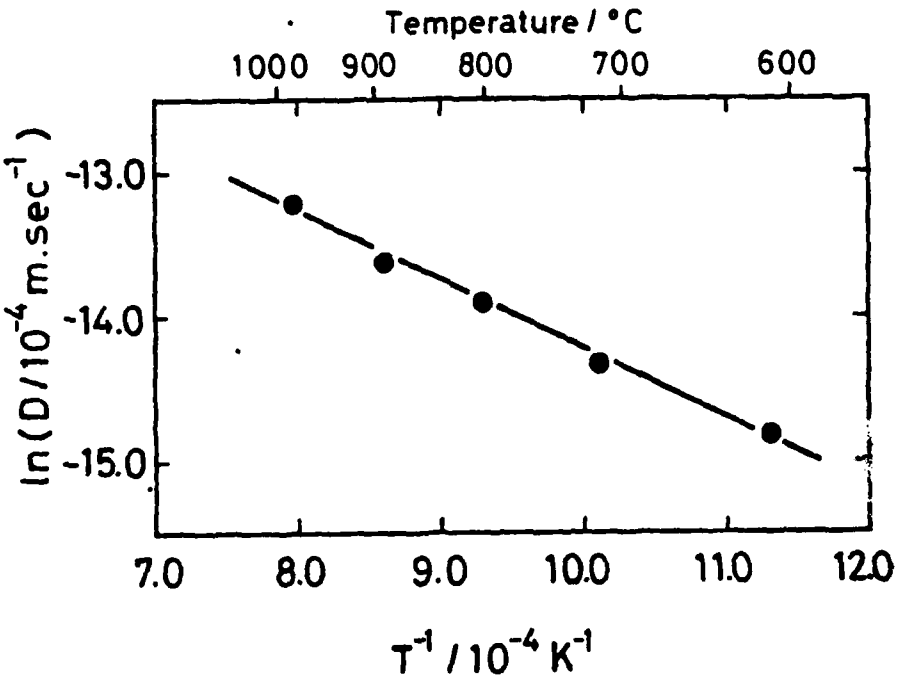

Figure 7 Plots of lnD vs. 1/T for Cr(III) in molten FLINAK.

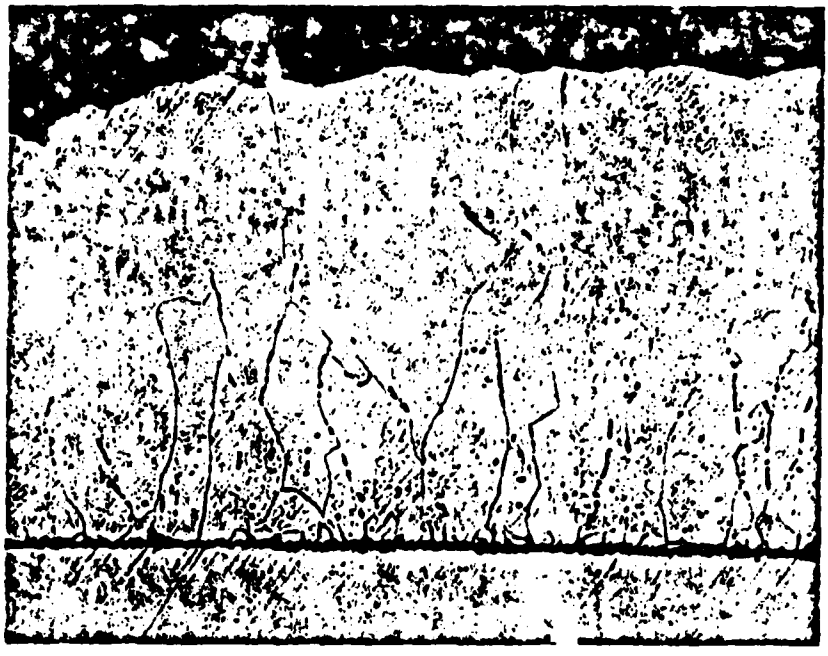

Figure 8 Chromium deposited on steel at 950°C, current density 20 ma cm^{-2}, 8% CrF_3, etched, x500 magnification.

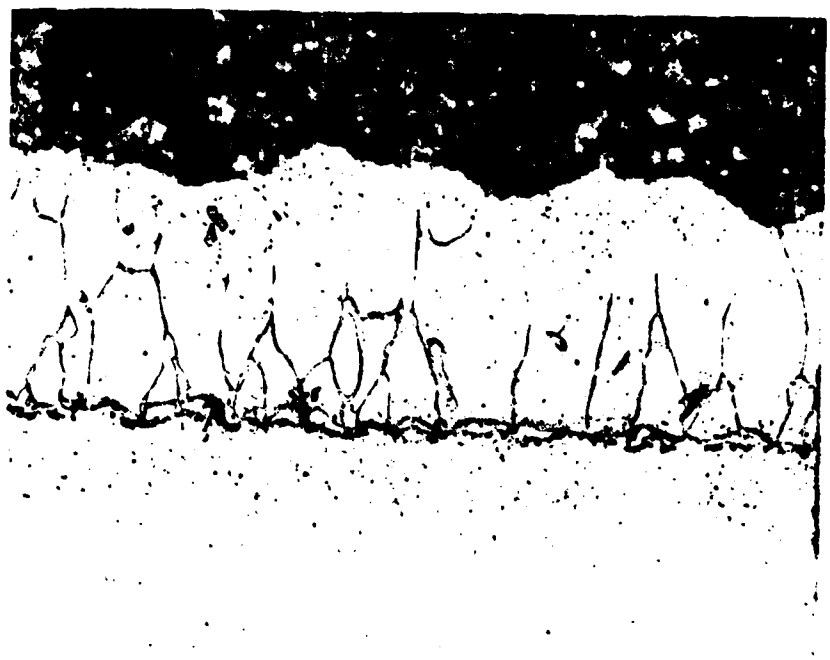

Figure 9 Chromium plated under conditions similar to the sample in Fig. 8, but on nickel-plated steel, X500 magnification.

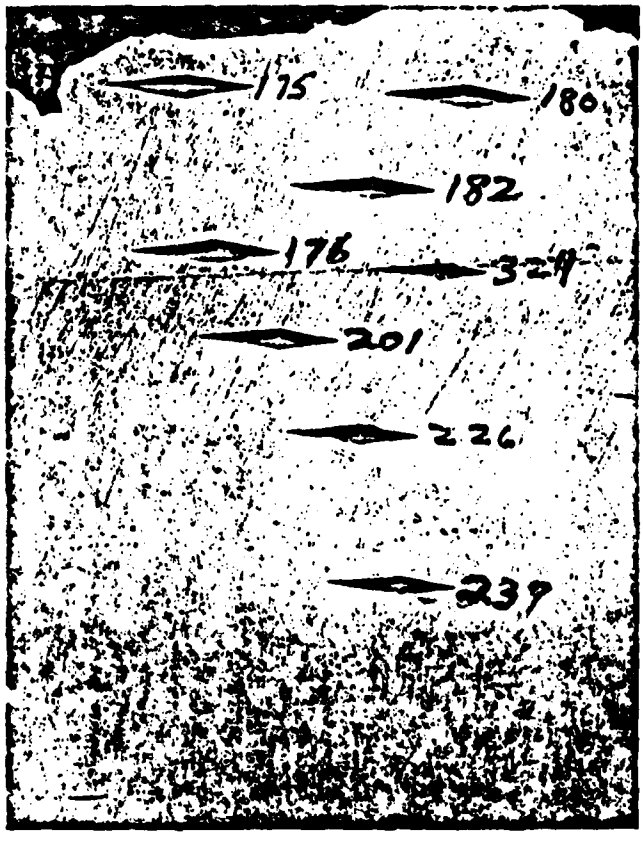

Figure 10. Hardness measurements on the chromium deposit shown in Fig. 8, x200 magnification.

Figure 11. Hardness measurements on Chromium deposited on steel at 900°C, 20 ma cm^{-2} current density, x300 magnification.

Figure 12. Hardness measurements in the chromium deposit shown in Fig. 10; x300 magnification.

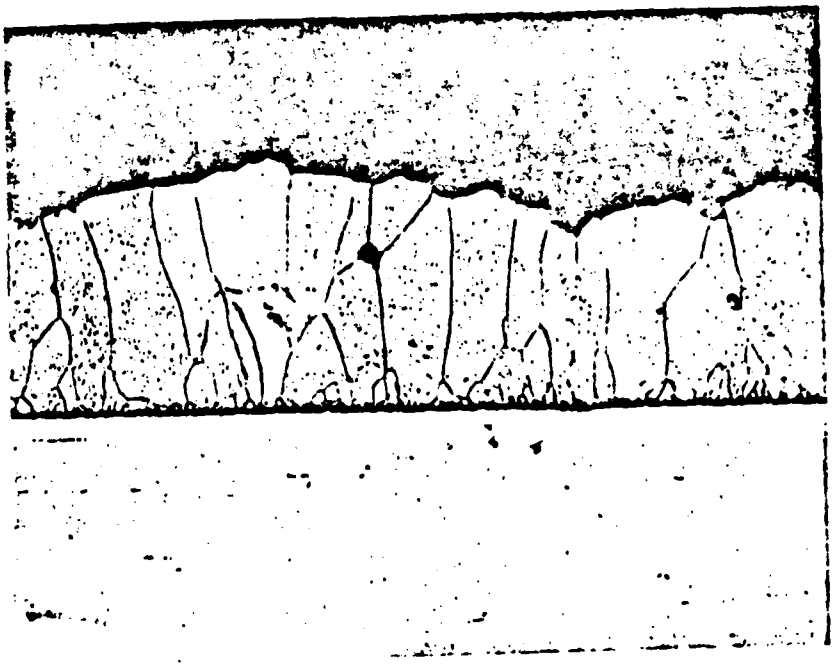

Figure 13. Chromium deposited on steel at 900°C, 20 ma cm^{-2} current density, x200 magnification.

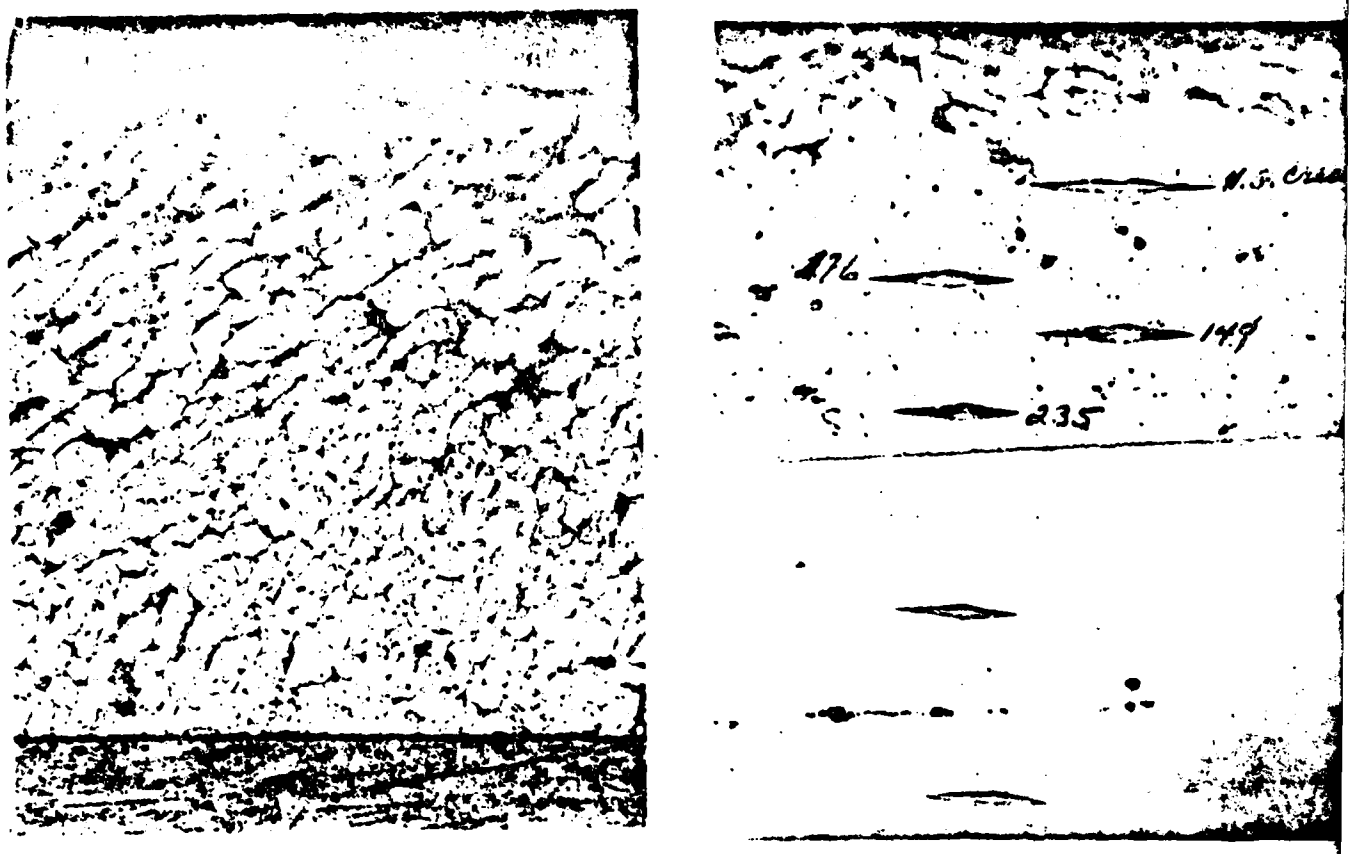

Figure 14. Chromium plated at 950°C from a bath containing 8% K_3CrF_6, 1% NiF_2, 25 ma cm^{-2} current density, left, eteched; x500 magnification; right, hardness measurements, x300 magnification.

Figure 15. Dendrite formation on chromium deposited at 950°C with a trace of NiF_2 in the bath; x30 magnification.

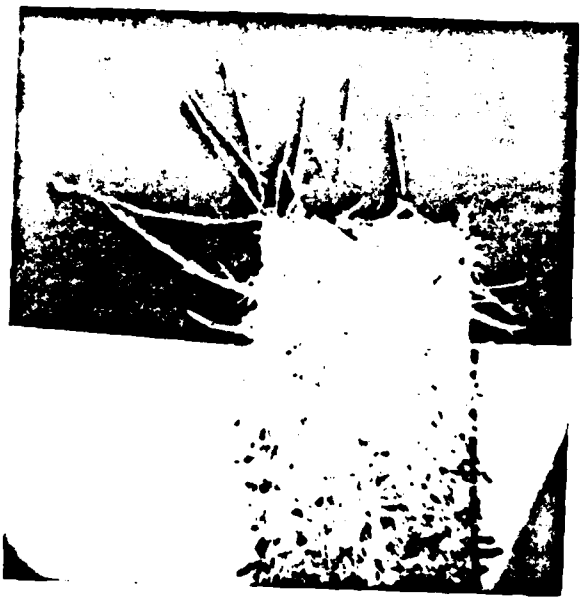

Figure 16. Needle-shaped dendrites formed when chromium is deposited from 8% K_3CrF_6-1% MnF_2.

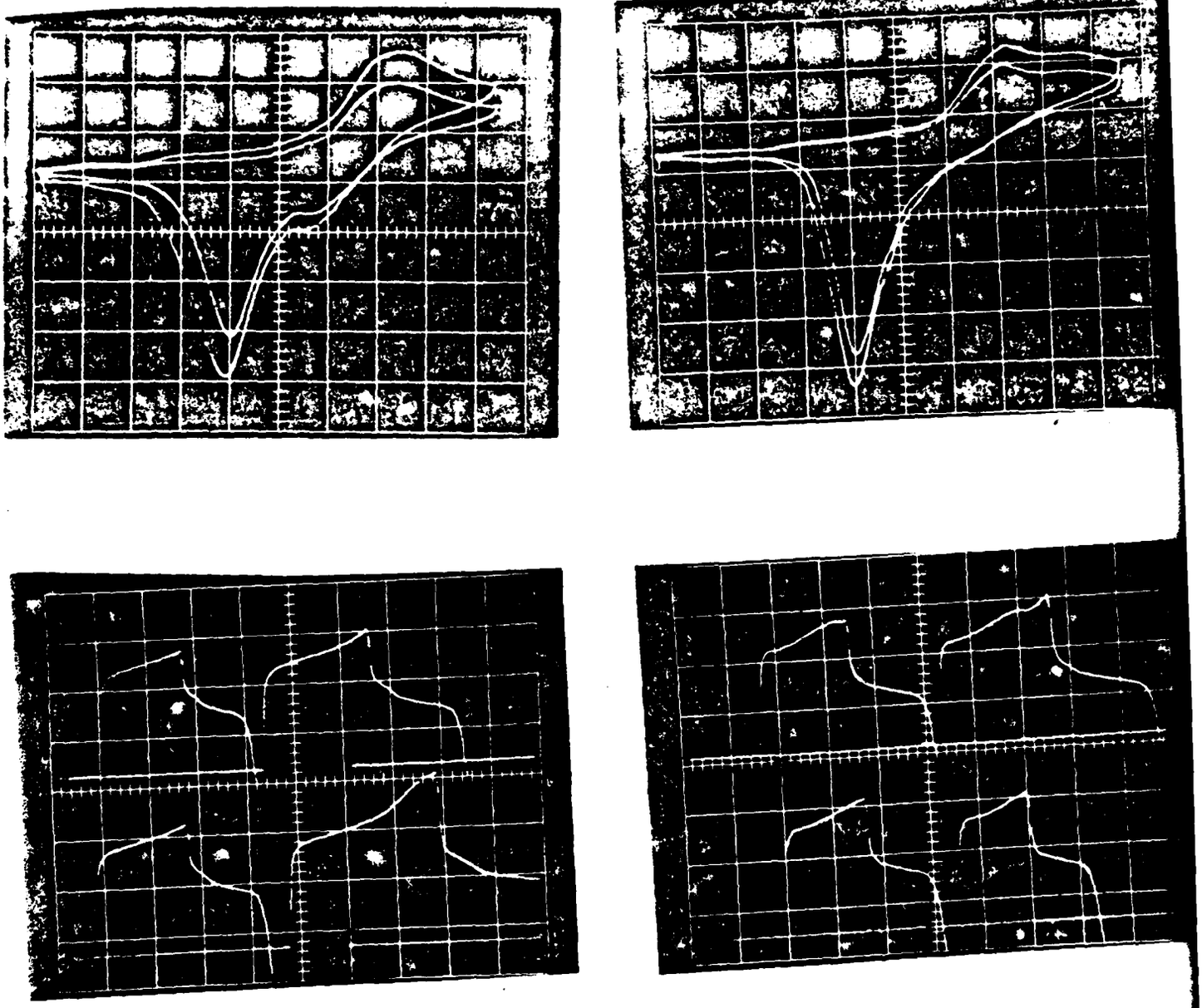

Figure 17. Upper: Cyclic voltammograms of Nb(V) in FLINAK.
Upper: Left, 950°C, Right, 750°C.
Lower: Chronopotentiograms of the same system.

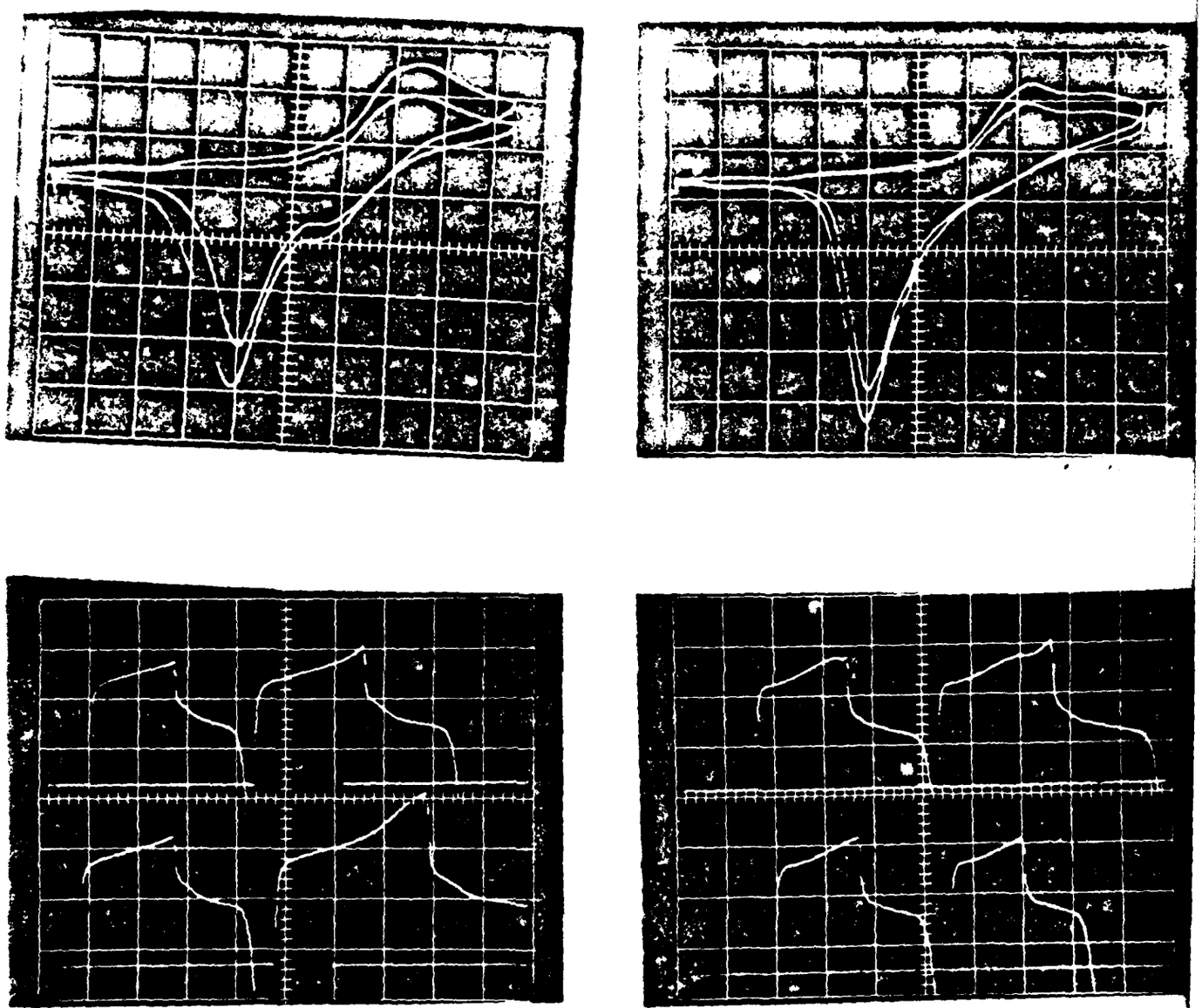

Figure 17. Upper: Cyclic voltammograms of Nb(V) in FLINAK.
Upper: Left, 950°C, Right, 750°C.
Lower: Chronopotentiograms of the same system.

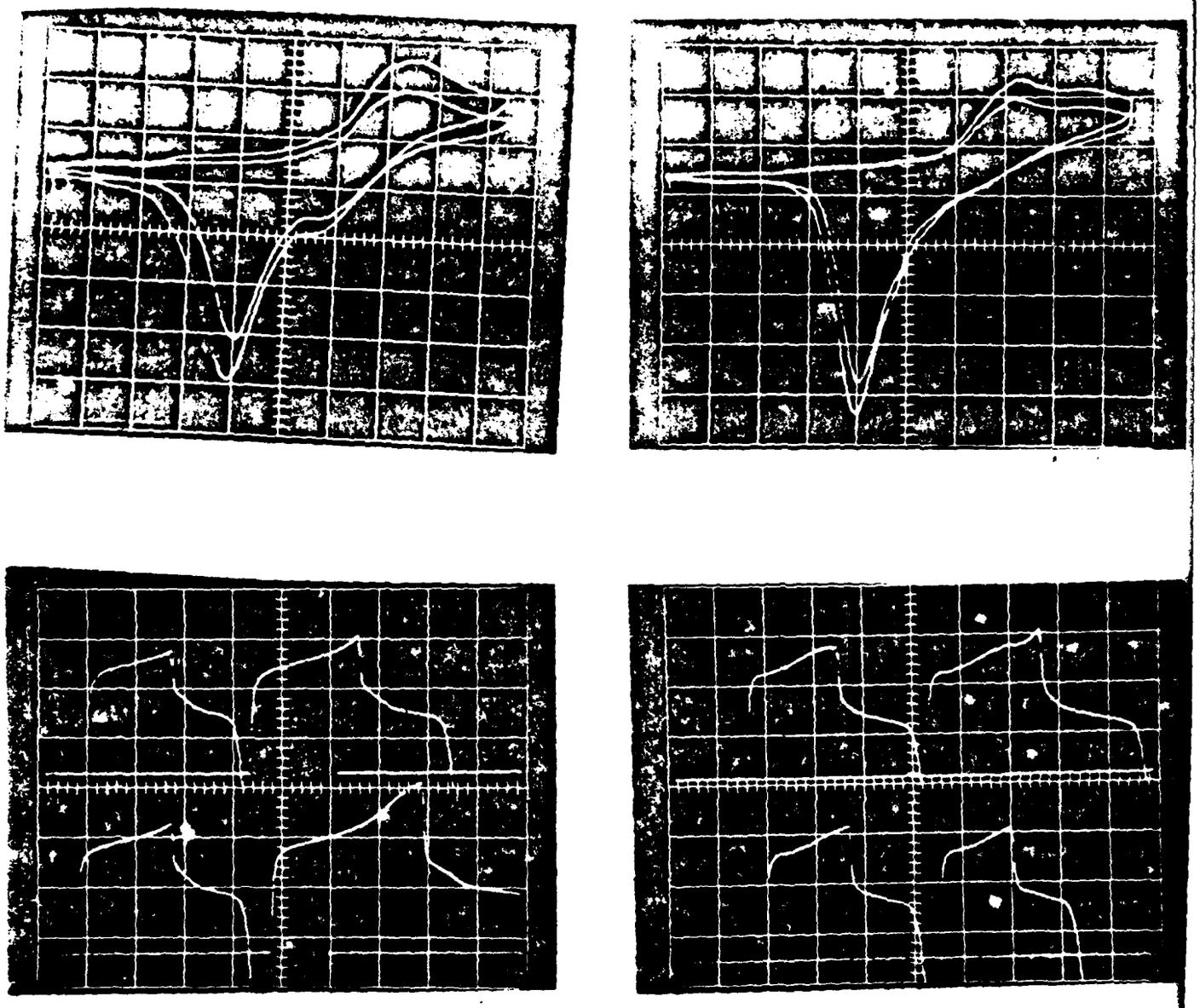

Figure 17. Upper: Cyclic voltammograms of Nb(V) in FLINAK.
Upper: Left, 950°C; Right, 750°C.
Lower: Chronopotentiograms of the same system.

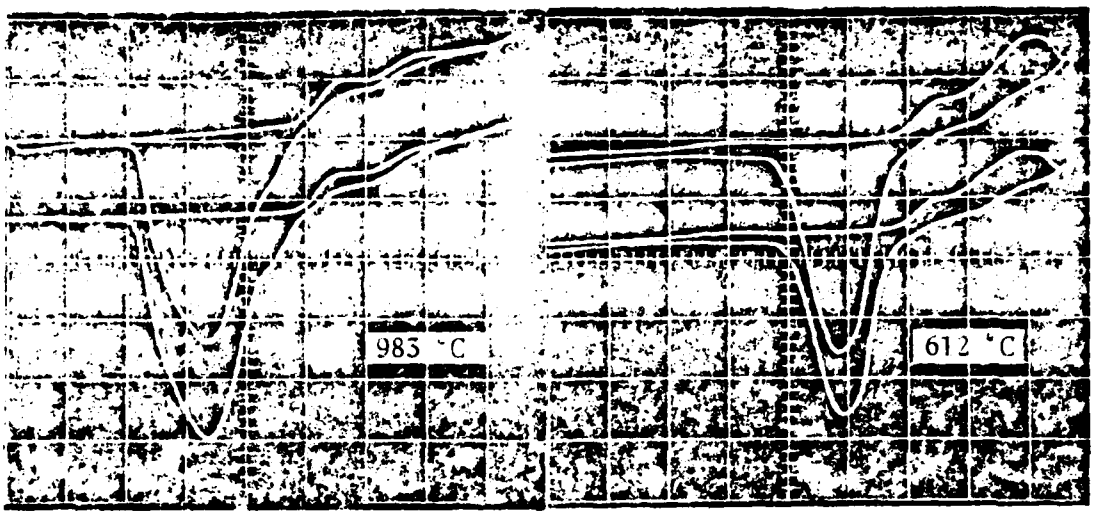

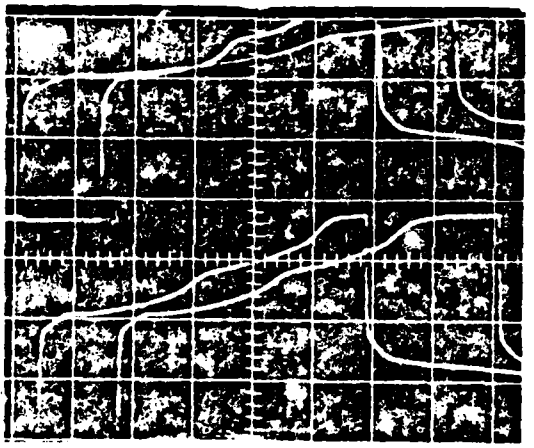

Figure 18. Upper: Cyclic voltammograms for the reduction of Ta^{5+} in molten FLINAK. (scan rate: 0.8, 0.5 V/sec; concentration of Ta^{5+} = 0.08 mol/l).

Lower: Chronopotentiograms for the reduction of Ta^{5+} in molten FLINAK (concentration of Ta^{5+} = 0.08 mol/l; 650°C).


DATE
FILME
5-8